Comparative Analysis of the Large and Small Signal Responses of "AC inductor" and "DC inductor" Based Chargers

Ilya Zeltser, *Student Member, IEEE* and Sam Ben-Yaakov, *Member, IEEE*

***Abstract*— Two approaches of operating inductors in switched mode power converters are compared.**

The classic method, utilized in most PWM converters, is to place the inductor in a path that has a non-zero average current. Such inductors are referred to here as "DC inductors". In contrast, inductors that operate with zero average current are denoted "AC inductors".

The theoretical analysis carried out in this paper compares the small signal response of the current in the DC and AC inductors as a function of various system parameters, such as input and output voltages and duty cycle, in the case of the DC inductor, and frequency in the case of the AC inductor. The analysis was supported by large and small signal model developed in this study and verified against analytically derived large and small signal equations. The small signal current response was derived by applying average models.

The analytical derivations and simulations of this study were verified experimentally. Good agreement was found between the theoretical predications and the analytical results.

Based on the results of this study one can conclude that "AC inductor" based topologies are optimal for current sourcing applications, such as battery chargers, where differences between the average input and output voltages are expected to exist and develop over time.

***Index Terms*—average model, DC-DC conversion, battery chargers, small-signal response.**

I. INTRODUCTION

The classic method, utilized in most PWM chargers, is to place an inductor in a branch that carries a non-zero average current [1]. Such inductors are referred to here as "DC inductors". In contrast, inductors that operate with zero average current are denoted "AC inductors". This latter operational method is similar to resonant load converters [2, 3] but in the topologies studied in this paper, a resonant capacitor is not applied [4] and the current waveforms are non sinusoidal [3-5]. The reason for the interest in AC inductor topologies is the fact that they achieve soft switching [3, 6-8]. The objective of this study was to compare the large and small signal responses of the currents in the DC and AC inductors and the output voltages, as a function of various system parameters, such as input voltage, output voltage and duty cycle perturbations in the case of the DC inductor, and as a function of frequency deviations in the case of the AC inductor.

The Authors are with the Power Electronics Laboratory, Department of Electrical and Computer Engineering, Ben-Gurion University of the Negev, Beer-Sheva, 84105, Israel (e-mail: sby@ee.bgu.ac.il). This research was supported by THE ISRAEL SCIENCE FOUNDATION (grant No. 113/02) and by the Paul Ivanier Center for Robotics and Production management.

II. LARGE SIGNAL ANALYSIS OF AC&DC INDUCTOR

To describe the behavior and delineate the differences between DC and AC inductor charger topologies, we first consider two DC-DC battery chargers shown in Fig. 1.

In both circuits, an output DC source approximates the battery and it is assumed that the input voltages are larger than the battery voltage. R_L represents the parasitic resistances of the inductor's branch.

DC inductor. The voltages applied to the main inductor of Fig. 1a are unipolar square wave signal V_D on the inductor's left terminal and constant DC voltage on its right terminal (Fig. 2). Neglecting the parasitic resistances of the inductor (R_L) as well as a voltage drop of the diode D_1 the duty cycle of the main switch is determined as:

$$D = \frac{V_{out}}{V_{in}} \tag{1}$$

The average value of the inductor's current and consequently the average power transferred cannot be controlled in this case solely by the duty cycle. That is, in order to regulate the power transferred to the load, an extra current control loop is mandatory. Without this extra current loop there is a risk of current runaway, as a result of a shift in the input or output averages.

AC inductor. It is assumed that the exemplary full-bridge inverter of Fig. 1b operates with 50% duty cycle and hence generates a symmetrical bipolar square wave signal at its output.

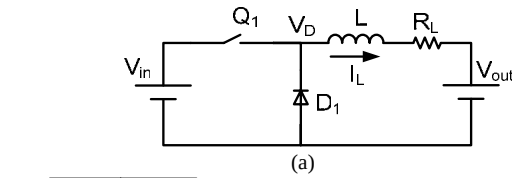

(a)

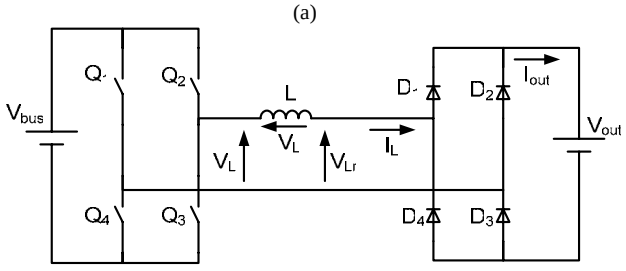

(b)

Fig. 1. Battery chargers. (a) Buck with DC inductor. (b) Full bridge with AC inductor.

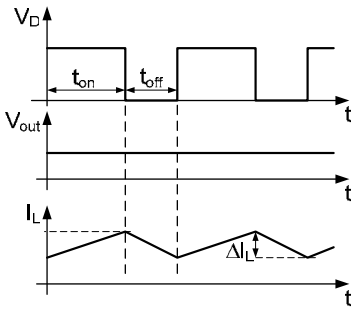

Fig. 2. Key waveforms of an ideal Buck converter.

In this case, the voltages applied to both terminals of the inductor in Fig. 1b are bipolar and the inductor's current flows in both directions (Fig. 3).

Due to the output diode bridge (Fig. 1b), the polarity of the voltage seen by the right terminal (V_{Lr}) of the inductor reverses every zero crossing of the inductor's current. During time interval t_1-t_2 (Fig. 3) the voltage at the input side of the inductor (V_{Ll}) is positive (V_{bus}), the inductor's current is positive and diodes D_1 and D_3 conduct. Consequently, net voltage seen by the inductor is positive and equal to (V_{bus}-V_{out}). The inductor's current is positive and increases. At t_2 the polarity of the input voltage switches. The current through the inductor keeps flowing in the same direction so diodes D_1, D_3 keep conducting. The voltage applied to the inductor will now be negative and equal to (-V_{bus}-V_{out}) and the inductor's current will start decreasing. At time instant t_3 the inductor's current crosses zero and its polarity reverses. As a result, diodes D_2 and D_4 turn on, the voltage seen by the right terminal of the inductor (V_{Lr}) is V_{out} and the net voltage applied to the inductor is (-V_{bus}+V_{out}). That is, the magnitude of the voltage applied to the inductor during the time interval t_3-t_4 is equal to that during t_1-t_2 but opposite in polarity. Similarly, the inductor's voltage during t_4-t_5 is equal in magnitude but opposite in polarity to that during t_2-t_3. Consequently, the current through the inductor reverses its polarity every input voltage switching cycle.

In the ideal case, the voltages seen by each inductor's terminal do not contain DC components. In practical AC inductor circuits, due to non-symmetry of the inverter's output voltage, a DC component may appear at the left terminal of the AC inductor (Fig. 1b).

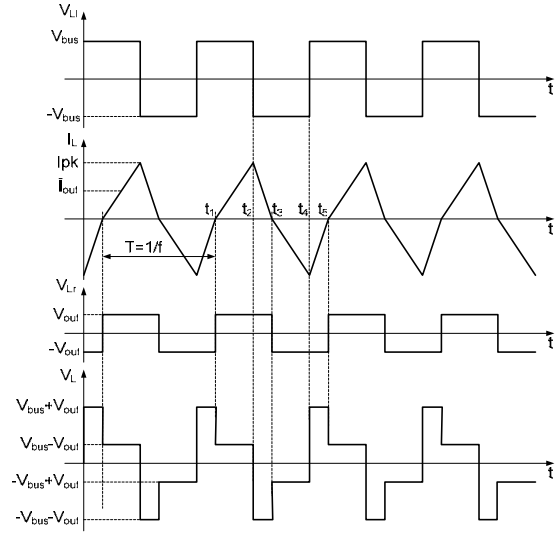

Fig. 3. Basic waveforms of the full bridge AC inductor converter.

This error component can be removed by a series capacitor, which of course cannot be applied in the DC inductor case.

During the time interval t_1-t_2 (Fig. 3) the peak inductor current Ipk is derived to be:

$$Ipk = \frac{V_{bus} - V_{out}}{L}(t_2 - t_1) \tag{2}$$

where L is the inductance of the inductor. Similarly, during the time interval t_2-t_3 Ipk is expressed as:

$$Ipk = \frac{V_{bus} + V_{out}}{L}(t_3 - t_2) \tag{3}$$

From (2) and (3), taking into account that (t_3-t_1) is half a switching cycle, yields:

$$(t_2 - t_1) + (t_3 - t_2) = I_{pk} L \frac{2V_{bus}}{V_{bus}^2 - V_{out}^2} = \frac{1}{2F} \tag{4}$$

where F is the switching frequency.

Rearranging (4) back for Ipk we get:

$$Ipk = \frac{V_{bus}^2 - V_{out}^2}{4LFV_{bus}} \tag{5}$$

The output current is the rectified inductor's current as depicted in (Fig. 4). Since the output current is of triangular shape, its peak value is twice its average value and hence:

$$\bar{I}_{out} = \frac{1}{2} Ipk = \frac{V_{bus}^2 - V_{out}^2}{8LFV_{bus}} \tag{6}$$

where $\bar{I}_{out}$ is the output current averaged over the switching cycle. The average power delivered to the output is thus:

$$P_{out} = \bar{I}_{out} \cdot V_{out} \tag{7}$$

Substituting (7) into (6) yields:

$$P_{out} = \frac{V_{out}}{8LF} \frac{V_{bus}^2 - V_{out}^2}{V_{bus}} \tag{8}$$

III. SMALL SIGNAL ANALYSIS

DC inductor. The average model approach described in [9] is used to analyze the small signal behavior of the system of Fig. 1a in open loop. That is, with a fixed duty cycle D. The average model of this system is shown in Fig. 5. $\bar{I}_L$ denotes an inductor's current averaged over the switching cycle.

Following the procedure described in [9], the small signal current response to a small signal injection in either input or output voltages, under constant duty cycle condition is found to be:

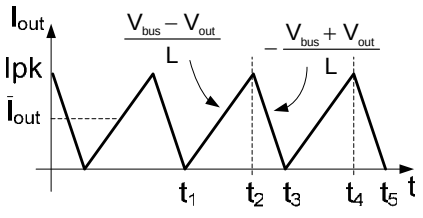

Fig. 4. Output current of an "AC inductor" converter.

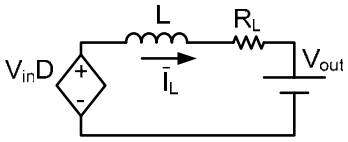

Fig. 5. Average model of a buck charger.

$$\frac{\bar{i}_L}{v} = \frac{K}{sL + R_L} \tag{9}$$

where $\bar{i}_L$ is the small signal average inductor current; *v* is a disturbance in either input or output voltage and K is equal to D in case of the input voltage or unity in case of the output voltage. According to (9), the slower the disturbance in the voltage the higher the ratio $\bar{i}_L / v$ is.

It implies that, for a constant D, even a small difference between the average voltages of the inductor's terminals may develop a very high current which will be limited only by parasitic resistances in the inductor's current path.

As mentioned above, the power transferred to the load is determined in case of DC inductor by controlling the average inductor's current (output current). The inductor's current can be controlled by designing a current feedback loop which will maintain the desired average current by modulating the duty cycle D. The design of a compensating network for this control loop requires knowledge of the small signal response of the inductor's current to the modulated (small signal changes) duty cycle D. This response was obtained using the average model of Fig. 5 after linearization, assuming that input and output voltages (V_{in} and V_{out} respectively) are constant (Fig. 6). The small signal current response to the modulation in the duty cycle is found to be:

$$\frac{\bar{i}_L}{d} = \frac{V_{in}}{sL + R_L} \tag{10}$$

where *d* is a small signal modulation of duty cycle D and $\bar{i}_L$ is a small signal change of the inductors current in response to this modulation.

Equation (10) implies that a small low frequency disturbance in the duty cycle D may invoke a large change in the inductor's current, which will be limited mainly by the parasitic resistance of the inductor.

AC inductor. Since the average current through the main inductor is zero we will focus on the average value of the output current which is the rectified inductor's current. During the time period t_1-t_2 (Fig. 4) the voltage applied to the inductor is (V_{bus}-V_{out}) whereas during t_2-t_3 it is –(V_{bus}+ V_{out}). Having in mind that (t_2-t_1)+(t_3-t_2)=1/2F the average voltage of the inductor will be given as:

$$\bar{V}_L = (V_{bus} - V_{out}) \cdot (t_2 - t_1) \cdot 2F - (V_{bus} + V_{out}) \cdot (t_3 - t_2) \cdot 2F \tag{11}$$

Equation (11) can be represented by the schematic diagram shown in Fig. 7.

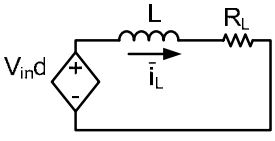

Fig. 6. A linearized average model of a DC inductor charger for constant input and output voltages.

Equating (2) and (3), we will find the ratio between the two time periods:

$$\frac{t_3 - t_2}{t_2 - t_1} = \frac{V_{bus} - V_{out}}{V_{bus} + V_{out}} \tag{12}$$

Expressing (t_3-t_2) as $\frac{1}{2F} - (t_2 - t_1)$ and substituting to (12) the time period (t_2-t_1) is found as follows:

$$(t_2 - t_1) = \frac{V_{bus} + V_{out}}{4V_{bus}F} \tag{13}$$

Considering (13), the expression for the left voltage source of Fig. 7 is reduced to $\frac{V_{bus}^2 - V_{out}^2}{2V_{bus}}$.

That is, the magnitude of the left voltage source is determined by input and output voltages. The right voltage source can be set to be a function of the output current and the switching frequency by applying (3).

From (3) the time period (t_3-t_2) duration is given as:

$$(t_3 - t_2) = \frac{LIpk}{V_{bus} + V_{out}} \tag{14}$$

Since the current is of a triangular shape (Fig. 4), the peak is twice its average value and hence:

$$(t_3 - t_2) = \frac{2L\bar{I}_{out}}{V_{bus} + V_{out}} \tag{15}$$

Applying (15) to the right voltage source of Fig. 7, the expression is rewritten as $4L\bar{I}_{out}F$.

The resulted average model is shown in Fig. 8.

A. Small signal current response to a disturbance in the input voltage.

We assume that the circuit is operated at some input voltage V_{bus}, output voltage V_{out}, and frequency F. The dependence of the inductor's current changes i_{out} on a small signal disturbance in input voltage V_{in} *(v_{in})* was found by linearizing the two depended sources of Fig. 8 and assuming that all variables except the input voltage are constant (Fig. 9):

$$\bar{i}_{out} = \frac{\frac{1}{2}\left(1 + \frac{V_{out}^2}{V_{bus}^2}\right) v_{in} - 4FL\bar{i}_{out}}{sL} \tag{16}$$

Taking into account the triangular shape of the inductor's current $\bar{i}_{out} = i_{out} / 2$ and rearranging:

$$\frac{i_{out}}{v_{in}} = \frac{K_1}{s + 4F} \tag{17}$$

where $K_1 = \frac{V_{bus}^2 + V_{out}^2}{V_{bus}^2 L}$.

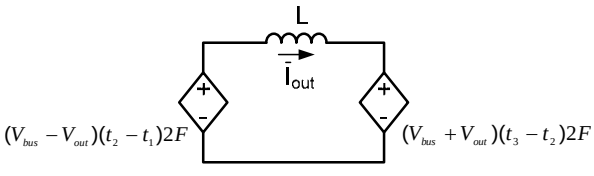

Fig. 7. Schematic diagram of equation (11).

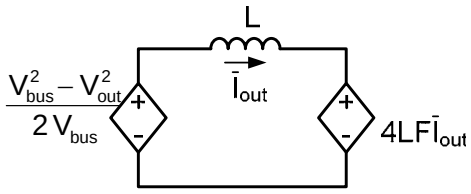

Fig. 8. Average large signal model of "AC inductor".

B. Small signal current response to a disturbance at the output voltage.

Following the same procedure as above but for the disturbance in the output voltage v_{out} , we find:

$$\frac{i_{out}}{v_{out}} = \frac{K_2}{s+4F} \qquad (18)$$

where $K_2 = -\frac{2V_{out}}{V_{bus}L}$.

Both (17) and (18) have finite response at low perturbation frequencies. That is, in contrast to the "DC inductor" case, the low frequency small signal current in the inductor will be limited by the inductor's impedance at the switching frequency (F) rather than by the low frequency impedance or the parasitic resistances.

C. Inductor's current response to a modulating frequency.

In an electronic charger it is usually desirable to maintain a constant load current. One possible way to achieve that will be to control the switching frequency. That is, the relevant control transfer function required for the design of the compensation network, is the response of the inductor's current to a modulation *f* in the switching frequency of the square-wave input voltage (F). To find this transfer function, the depended sources of Fig. 8 were linearized assuming that the disturbance was in the switching frequency (Fig. 10). All the voltage sources were assumed to be constant. The small signal output current was found to be:

$$\bar{i}_L = \frac{-(4L\bar{I}_{out} f + 4L\bar{i}_{out} F)}{sL} \qquad (19)$$

Taking into account again that $\bar{i}_{out} = i_{out}/2$ and rearranging:

$$\frac{i_{out}}{f} = \frac{8I_{out}}{s+4F} \qquad (20)$$

Fig. 11 shows the Bode diagram of (20) plotted for L= 75µH, V_{bus}=200V, V_{out}=50V, and F=62.5kHz.

The last expression implies that for low frequencies the inductor behaves as a resistor (flat response in the bode diagram of Fig. 11).

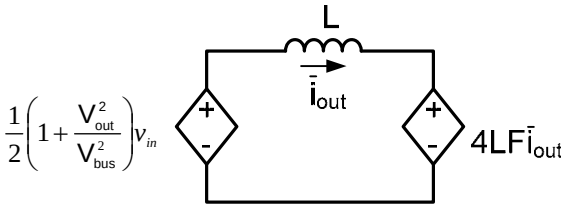

Fig. 9. Average small signal model of AC inductor charger linearized for a constant output voltage

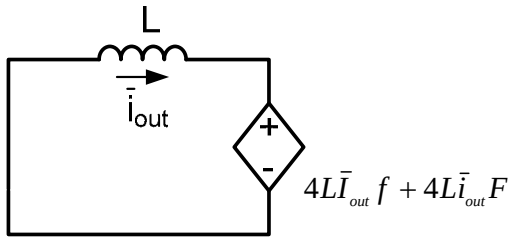

Fig. 10. Linearized average small signal model of AC inductor for small-signal injection in F, (*f*).

That is, even for a very slow disturbance in the switching frequency (very slow modulation of F) the changes in the inductor's current will be negligibly small considering a practical switching frequency (tens of kilohertz).

It follows that the AC inductor charger, unlike the case of the DC inductor case, can be operated in open loop. This is a corollary of the fact that the AC inductor behaves as a current source while the DC inductor behaves as a voltage source.

IV. EXPERIMENTAL

The AC inductor case was tested experimentally using a half bridge topology with a blocking capacitor (Fig. 12). The battery load was modeled in the experimental setup by an RC network with very long time constant so it can be considered practically zero impedance at the tested small signal frequencies. The inductor was 75µH, load capacitor 4700µF, and load resistor 25Ω. DC blocking capacitor was (1.5mF). The bus voltage was 100VDC. Output voltage was about 50VDC. The switching frequency was set to 62.5kHz (125kHz at the load side) and power transferred to the load was about 100W.

Fig. 13 shows the response of the output current to the disturbance at the output voltage. The output voltage was modulated by adding a 50Hz ac voltage source in series with the RC network.

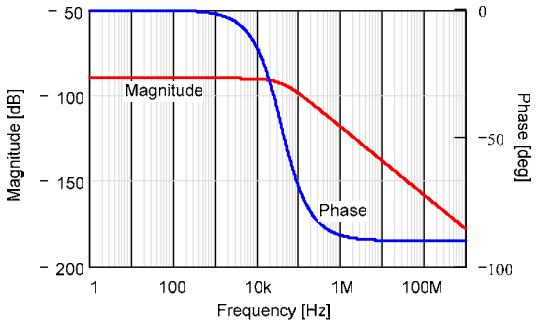

Fig. 11. Bode diagram of output current to switching frequency modulation transfer function (20).

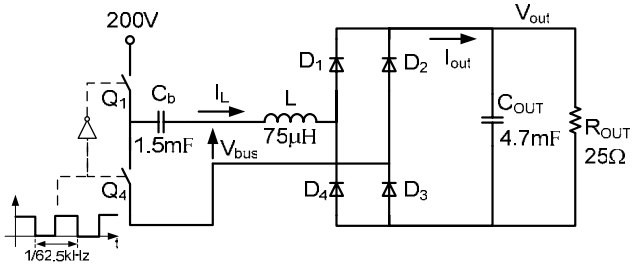

Fig. 12. Experimental setup.

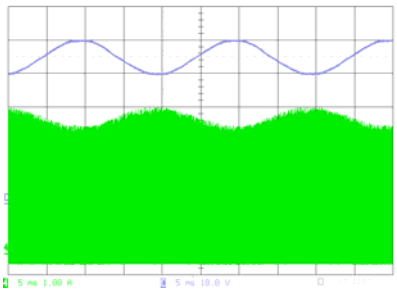

Fig. 13. Output current response to output voltage modulation. Upper trace: Modulating voltage 10V/div; Lower trace: Output current 1A/div; Horizontal scale: 5ms/div.

The injected signal had an amplitude of $10V_{pk\text{-}pk}$. This resulted (Fig. 13) in an envelope amplitude of the inductor current of about $0.55A_{pk\text{-}pk}$. By substituting f of 50Hz, v_{out} of 10V into (18) we get the value of 0.54A which is in good agreement with the measured value.

Output current response to a modulated switching frequency is presented in Fig. 14. The frequency was modulated by a 1kHz sinusoidal modulating signal. Maximum frequency deviation was 10kHz (modulation index of 10). The measured current to frequency ratio was about 66[μA/Hz]. The ratio calculated from (20) is 64[μA/Hz].

An expanded view of the output current, modulating signal as well as the voltage across the inductor is shown in Fig. 15.

The results of present study show that "AC inductors" are less sensitive to average voltage disturbances at either input or output side. As a result, they can be operated as current sources in open loop configuration without the need for current feedback. On the other hand, in the case of the "DC inductor" a small difference between the average voltages of the inductor's terminals may cause current run-away and therefore, a tight current feedback loop must be applied.

The analytical derivations and simulations of this study were verified experimentally. Good agreement was found between the theoretical predications and the analytical results.

V. DISCUSSION AND CONCLUSIONS

Based on the results presented in this study one can conclude that "AC inductor" based topologies are optimal for current sourcing applications, such as battery chargers, where differences between the average input and output voltages are expected to exist and develop over time.

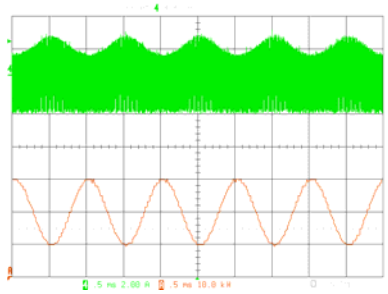

Fig. 14. Output current response to modulation of switching frequency. Upper trace: Output current 2A/div; Lower trace: Modulating frequency 10kHz/div; Horizontal scale: 0.5ms/div.

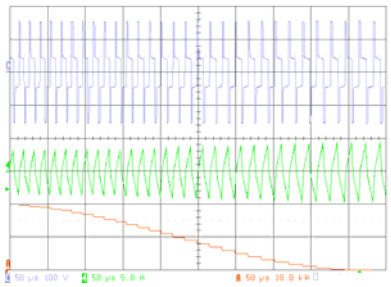

Fig. 15. Expanded view of AC inductor's key waveforms. Upper trace: Inductor's voltage: 100V/div. Middle Trace: Inductor's current 5A/div. Lower Trace: Switching frequency 10kHz/div (carrier frequency 62.5kHz). Horizontal scale: 50us/div

The disadvantage (from the dynamics point of view) is the higher output impedance, similar to the case of a DC inductor converter with an inner current loop.

REFERENCES:

[1] R. W. Erickson, "Converter circuits," chap. 6 in *Fundamentals of Power Electronics*, Chapman&Hall, N.Y., 1997.

[2] R. W. Erickson, "Resonant Conversion," chap. 19 in *Fundamentals of Power Electronics*, Chapman&Hall, N.Y., 1997.

[3] S. Sato, S. Moisseev, and M. Nakaoka, "A novel synchronous rectifiers based ZVS-PWM DC-DC power converter with extended soft-switching operational range," *IEEE The 25th International Telecommunications Energy Conference, INTELEC'03, pp. 268-273, 19-23 October 2003.*

[4] Y. Zhang, P. C. Sen, "A new ZVS phase-shifted PWM DC-DC converter with push-pull type synchronous rectifier," IEEE Canadian Conference on Electrical and Computer Engineering, CCECE 2003, vol. 1, pp. 395-398, 4-7 May 2003.

[5] F. Krismer, J. Biela, and J. W. Kolar, "A Comparative Evaluation of Isolated Bi-directional DC/DC Converters with Wide Input and Output Voltage Range," *IEEE Industry Applications Conference, Fourteenth IAS Annual Meeting, vol. 1, pp. 599 - 606, 2-6 October 2005.*

[6] C. Hang-Seok, J.H. Lee, B. H. Cho, J. W. Kim, "Analysis and design considerations of zero-voltage and zero-current-switching (ZVZCS) full-bridge PWM converters," *IEEE 33rd Annual Power Electronics Specialists Conference, PESC 2002, vol. 4, pp. 1835-1840, 23-27 June 2002*.

[7] M. Xu, Y. Ren, J. Zhou, and F. C. Lee, "1-MHz Self-Driven ZVS Full-Bridge Converter for 48V Power Pod and DC/DC Brick," *IEEE Transaction on Power Electronics, vol. 20, pp. 997-1006, 2005*.

[8] S. TingTing, H. Nianci, "A novel zero-voltage and zero-current-switching full-bridge PWM converter," *Eighteenth Annual Applied Power Electronics Conference, APEC 2003, vol. 2, pp. 1088-1092, 2003*.

[9] S. Ben-Yaakov, "Average simulation of PWM converters by direct implementation of behavioral relationships," *International Journal of Electronics, vol. 77, pp. 731-746, 1994.*